Generating a Photonic Dimer for Use in a Two-Qubit Photonic Quantum Gate

James Kennedy

Introduction

In classical computing, the information contained in a single bit can be represented as either a logical 0 or 1. In quantum computing, the information contained in a single qubit can be represented as a mixture, or superposition, of 0 and 1 simultaneously. Moreover, the information contained in one qubit can become strongly correlated with the information contained in one or more different qubits; these qubits are then referred to as entangled. Entangled qubits theoretically allow the representation of states that are too complex to be simulated efficiently by a classical computer.[2] By exploiting quantum mechanical phenomena such as superposition and entanglement, scientists hope to leverage quantum computers to solve problems that are currently intractable for classical computers. These problems include the modeling of quantum mechanical systems, the optimization of complex cost functions, and various problems related to cryptography.[7]

While quantum computing promises to provide exponential speedup over classical computers for select applications, it also faces tremendous technological challenges. The state of a qubit is incredibly fragile. If disturbed, the state of a qubit in superposition may collapse to either a classical 0 or 1, in which case any advantage conferred by quantum computing is lost. Qubits also possess an additional property known as phase, which allows qubits to interfere constructively and destructively with one another. Random noise from the environment threatens to perturb both the superposition and phase of a qubit, which may cause information to become irreparably lost during computation. The loss of information contained in a qubit due to the environment is known as decoherence.[12] In an effort to stave off decoherence, qubits are frequently maintained at temperatures near absolute zero or in a vacuum.[6] Various error correction codes (e.g., Shor code, Steane code) are designed to allow quantum computers to

preserve information even when errors inevitably occur. Designing fault-tolerant quantum computers remains an open problem.[7]

Photonics comprises one of several promising architectures for quantum computing alongside trapped ions, transmon qubits, and others.[5] In photonic quantum computing, the information contained in a single qubit is encoded in one or more degrees of freedom of a photon. These degrees of freedom include the photon's path, polarization, time, and frequency.[6] Photons are especially appealing as carriers of quantum information because they travel at the speed of light, barely interact with their environment (resulting in longer coherence times), and do not need to be kept at temperatures near absolute zero to preserve their state.[2] However, qubits must be able to do more than simply hold state. To produce any sort of useful computation, it must also be possible to manipulate the information contained in a qubit. To this end, scientists apply operations known as quantum gates to manipulate the state of one or more qubits. A small set of single-qubit quantum gates and an appropriately chosen two-qubit quantum gate are sufficient to implement any quantum algorithm.[8] The implementation of a quantum gate varies depending on the architecture. Advantageously, single-qubit photonic quantum gates are trivially implemented with linear optical elements such as beam splitters and waveplates. For example, a beam splitter can be used to change a photon's path, and a waveplate can be used to change a photon's polarization. However, two-qubit photonic quantum gates are notoriously difficult to implement; not only do photons barely interact with their environment, but they also barely interact with other photons.[5] Nonetheless, two-qubit quantum gates are critical to the development of quantum computers. Unlike single-qubit quantum gates, two-qubit quantum gates cannot be efficiently simulated by a classical computer. The exponential speedup promised by quantum computers necessitates the realization of two-qubit quantum gates.[2]

The Nanophotonics and Nanofabrication Group is working towards developing a two-qubit photonic quantum gate. Specifically, the group is working towards developing a

controlled-phase gate, which conditionally changes the phase of a target qubit depending on the state of a control qubit. The successful operation of this gate depends on the generation of a two-photon bound state known as a photonic dimer.[2] A photonic dimer is generated when two photons interact with a quantum dot that is chirally coupled to a waveguide. A quantum dot is a nanoparticle or nanocrystal of semiconducting material that absorbs photons and subsequently emits photons at discrete frequencies. Although the emission of a quantum dot is symmetric under normal circumstances, a quantum dot that is chirally coupled to a waveguide will only emit light in one direction in the waveguide. Verifying the generation of a photonic dimer requires a complex experimental setup that involves a quantum dot embedded within a photonic crystal, waveguides, input / output grating couplers, and a phase modulator arranged in a Mach-Zehnder interferometer.[3] Experiments must be performed to confirm the correct operation of these individual components before assembling the complete setup. Performing experiments entails setting up the necessary equipment, optimizing signal collection paths, and recording and analyzing data among other tasks.

Objectives

The primary goal of this research is to generate a photonic dimer. The long-term goal of this research is to use the photonic dimer to demonstrate the correct operation of a two-qubit photonic quantum gate. To attain these goals, several problems have to be addressed along the way. The first of these problems is the verification of the quantum dot, which entails measuring the emission spectrum of the quantum dot and capturing the dependence of this emission spectrum on the applied bias voltage and laser power. The second of these problems is the verification of the waveguide and input / output grating couplers, which entails imaging an integrated waveguide and observing the transmission of a near-infrared laser through said waveguide. The third of these problems is the verification of additional components (e.g., photonic crystal, phase modulator) and the assembly of these components into a Mach-Zehnder

interferometer. The fourth and final of these problems is using the Mach-Zehnder interferometer to generate a photonic dimer. Over the course of this project, the first two problems were successfully addressed. The remaining two problems still need to be addressed in future research.

Methods

The first major milestone was to confirm the correct operation of the quantum dot. Theory dictated that exciting the quantum dot with a near-infrared laser should cause the quantum dot to emit light at discrete frequencies also in the near-infrared regime. To measure the emission spectrum of the quantum dot, it was necessary to calibrate a spectrometer to detect near-infrared light. The key components of the spectrometer in the lab are the entrance slit, the diffraction grating, and a CCD camera.[10] These components are housed in the body of the spectrometer, which is concealed under a black tarp to block any stray light from the environment. The spectrometer measures the emission spectrum of whatever signal enters at the entrance slit. From the entrance slit, the signal propagates to the diffraction grating. The diffraction grating separates the signal into its spectral components by reflecting different wavelengths at different angles. These spectral components propagate to the CCD camera where they are digitized and read out to a computer. If the spectrometer is calibrated properly, a monochromatic signal should correspond to a sharp peak in the emission spectrum. Sharp peaks allow a user to differentiate between spectral components that have similar wavelengths. If the spectrometer is not calibrated properly, then peaks may broaden and spectral components with similar wavelengths may appear to blend into one another. To calibrate the spectrometer, a near-infrared laser (which is itself a monochromatic signal) was passed through the entrance slit. A series of lenses and mirrors were used to focus the near-infrared laser to a point at the entrance slit, which in turn causes the laser to be focused to a point at the CCD camera. These lenses and mirrors were adjusted to make the corresponding peak in the emission spectrum

appear as sharp as possible. The emission spectrum of the near-infrared laser as captured by the calibrated spectrometer is shown in Figure 1.

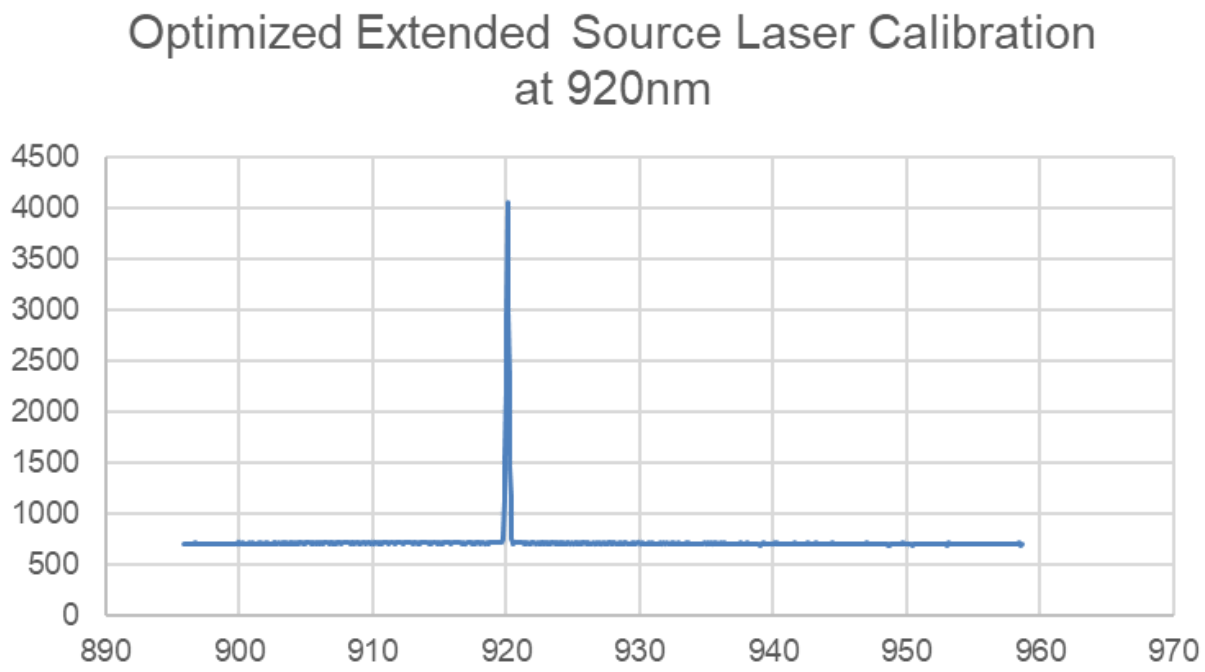

Figure 1: Emission spectrum of a 920 nm wavelength laser. Horizontal axis is wavelength in nm. Vertical axis is counts recorded during the exposure time. The laser produces a sharp peak whose full width at half maximum is less than 0.5 nm, which is indicative of a spectrometer that has been calibrated very well for detecting near-infrared light.

To measure the emission spectrum of the quantum dot, it was also necessary to employ the use of a cryostat. A cryostat is a vacuum insulated chamber that can lower its internal temperature (and the temperature of any sample contained within) to near absolute zero.[11] The cryostat in the lab uses liquid helium to achieve these ultra-low temperatures. In order to observe the characteristic discrete emission spectrum of the quantum dot, the quantum dot had to be loaded into the cryostat. At low temperatures, the quantum dot only occupies a small number of energy states; therefore, the number of possible state transitions (and hence the

number of possible energies / frequencies of emitted photons) is few and well-controlled, resulting in a discrete emission spectrum. At high temperatures, the quantum dot can occupy a large number of energy states; therefore, the number of possible state transitions is many and uncontrolled, resulting in a continuous emission spectrum.

With the spectrometer calibrated and the quantum dot loaded into the cryostat, the next step was to excite the quantum dot with a laser and collect the emission. The laser originated from a box and needed to be routed to the cryostat at the other end of the lab. The emission originated from the quantum dot in the cryostat and needed to be routed to the spectrometer at a different table. The primary optical components to route signals around the lab included mirrors, lenses, beam splitters, and fiber optic cables. Mirrors reflect incident signals and can rotate on two axes, allowing both coarse and fine adjustments to the signal paths. Lenses focus or disperse a signal through refraction, allowing the width of a signal beam to be carefully controlled. Beam splitters allow half of the power in a signal to proceed unobstructed while simultaneously redirecting the other half of the power in a manner similar to a mirror, allowing the design of more complex signal paths. Lastly, fiber optic cables allow the routing of signals over long distances (e.g., between tables or across the lab). The laser path and emission path as they appear in the experimental setup positioned above the cryostat are shown in Figure 2.

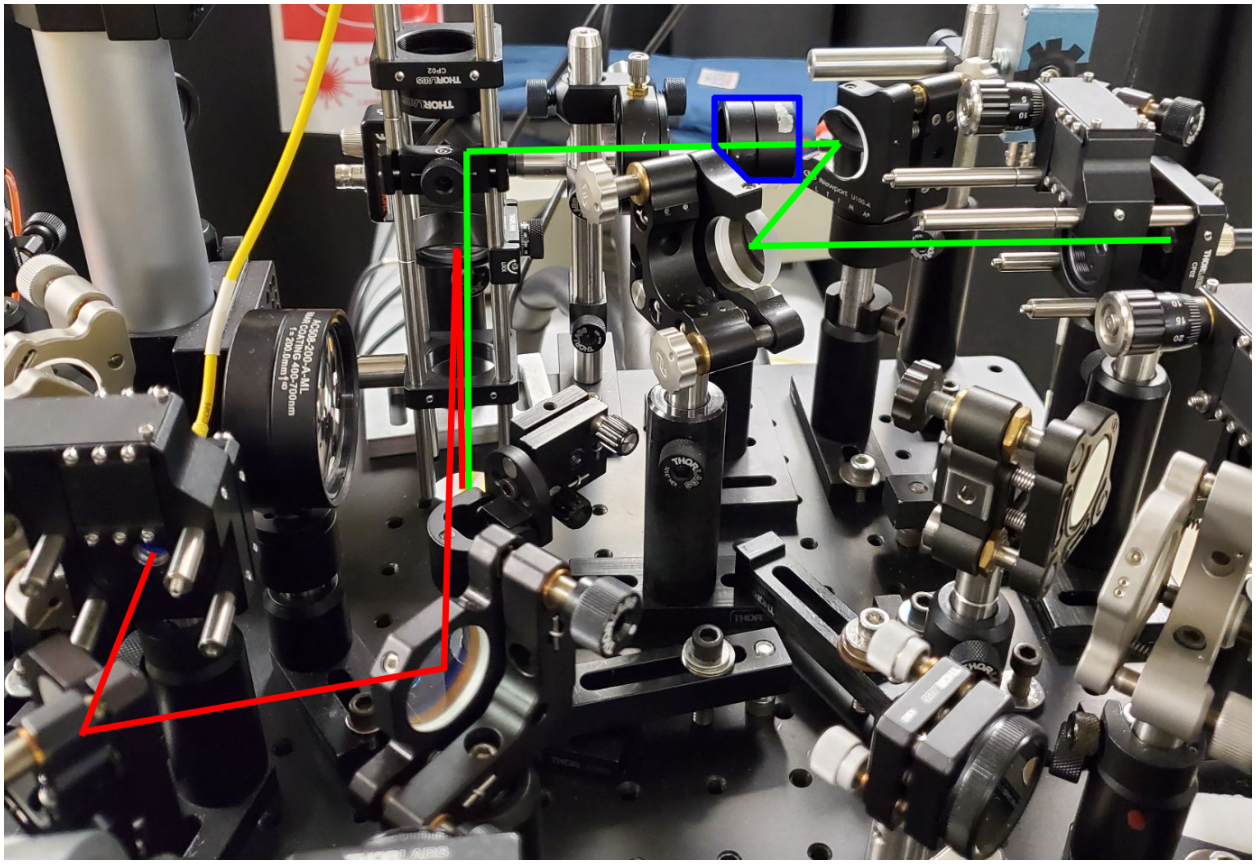

Figure 2: Experimental setup positioned above the cryostat. Laser enters the setup from the yellow fiber optic cable on the left and follows the red path into the cryostat. The laser excites the quantum dot within the cryostat, and the emission from the quantum dot follows the green path. The quantum dot emission leaves the setup through an orange fiber optic cable on the right, which routes the emission to the spectrometer at a different table. The component outlined in blue is a longpass filter.

Having established the signal paths, the quantum dot was excited with a laser, and the collected emission was recorded at the spectrometer. The quantum dot was embedded within a sample between layers of GaAs and InAs. GaAs and InAs also exhibit photoluminescence, or the emission of photons following the absorption of photons. As a result, the collected emission included the emission spectra of GaAs and InAs in addition to the emission spectrum of the

quantum dot. Unlike the emission spectrum of the quantum dot, the emission spectra of GaAs and InAs are continuous and broad. The emission spectra of GaAs and InAs are also much higher intensity and therefore much easier to detect using the spectrometer. The emission spectrum of GaAs was detected first, followed by the emission spectrum of InAs. The emission spectrum of InAs was used to optimize the signal collection path. The positions and orientations of mirrors and lenses along the collection path were adjusted until the emission spectrum of InAs was as strong as possible. The position of the quantum dot within the cryostat was also adjusted using a piezoelectric stage that allowed translation along three axes. After detecting the emission spectrum of InAs, the emission spectrum of the quantum dot was still nowhere to be found. The wavelength of the laser was increased to avoid exciting the InAs and GaAs layers while still exciting the quantum dot. Longpass filters were also added to the signal collection path to attenuate signals other than the quantum dot emission spectrum. After further optimizations to the signal collection path, the emission spectrum of the quantum dot was finally observed at the spectrometer. The emission spectrum of the quantum dot is shown in Figure 3.

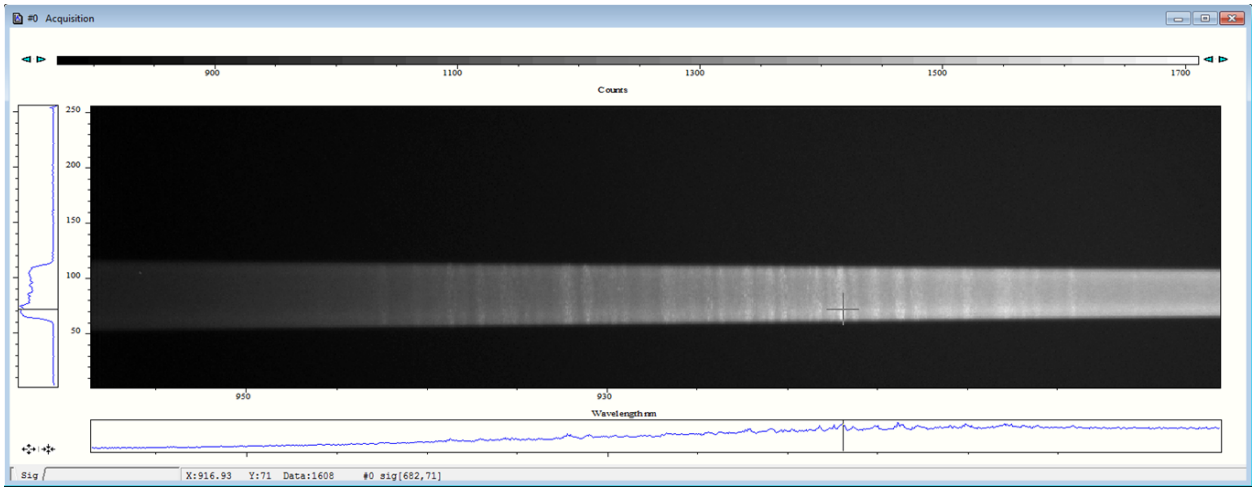

Figure 3: Emission spectrum of the quantum dot as recorded by the spectrometer. The broad white band is background noise. The desired signal is actually the narrow, vertical stripes superimposed on top of the white band. The number of these stripes suggests

that the laser is exciting multiple quantum dots. These stripes are in the near-infrared spectrum, hence why the spectrometer was previously calibrated for near-infrared light.

Once the emission spectrum of the quantum dot was observed at the spectrometer, the next step was to determine the response of the emission spectrum to a variable applied bias voltage and a variable laser power. A power supply connected to the cryostat was used to apply a bias voltage to the sample. The magnitude of the applied bias voltage was determined according to the display on the power supply. A neutral density filter was inserted into the laser path to control the laser power. The magnitude of the laser power was determined according to a power meter. First, the laser power was held constant at 170 μW while the applied bias voltage was swept from 0 V to 1.7 V in 0.5 V increments. At each increment, the emission spectrum of the quantum dot was recorded. Next, the applied bias voltage was held constant at 1.3 V while the laser power was swept from 0 μW to 1500 μW in 50 μW increments. At each increment, the emission of the quantum dot was recorded. To isolate the quantum dot emission spectrum from noise as much as possible, the lights in the lab were turned off while collecting data and the exposure time at the spectrometer was increased to two minutes. The response of the emission spectrum to the applied bias voltage and laser power confirmed that it belonged to the quantum dot. Thus, the quantum dot had been verified to a satisfactory extent.

The second major milestone was to confirm the correct operation of the waveguides and input / output grating couplers. To reach this milestone, a second experimental setup was created separate from the experimental setup used to verify the quantum dot. This second experimental setup is shown in Figure 4. In this second experimental setup, white light from a lamp illuminated a sample underneath a custom lens mount. The scattering of this white light off the sample was collected by a portable CCD camera positioned overhead. Initially, the sample placed underneath the custom lens mount was a simple patterned sample used to optimize the experimental setup. Specifically, the lenses in the experimental setup were adjusted until the

patterns on the sample came into focus in the CCD camera image. These patterns were approximately 100 microns across.

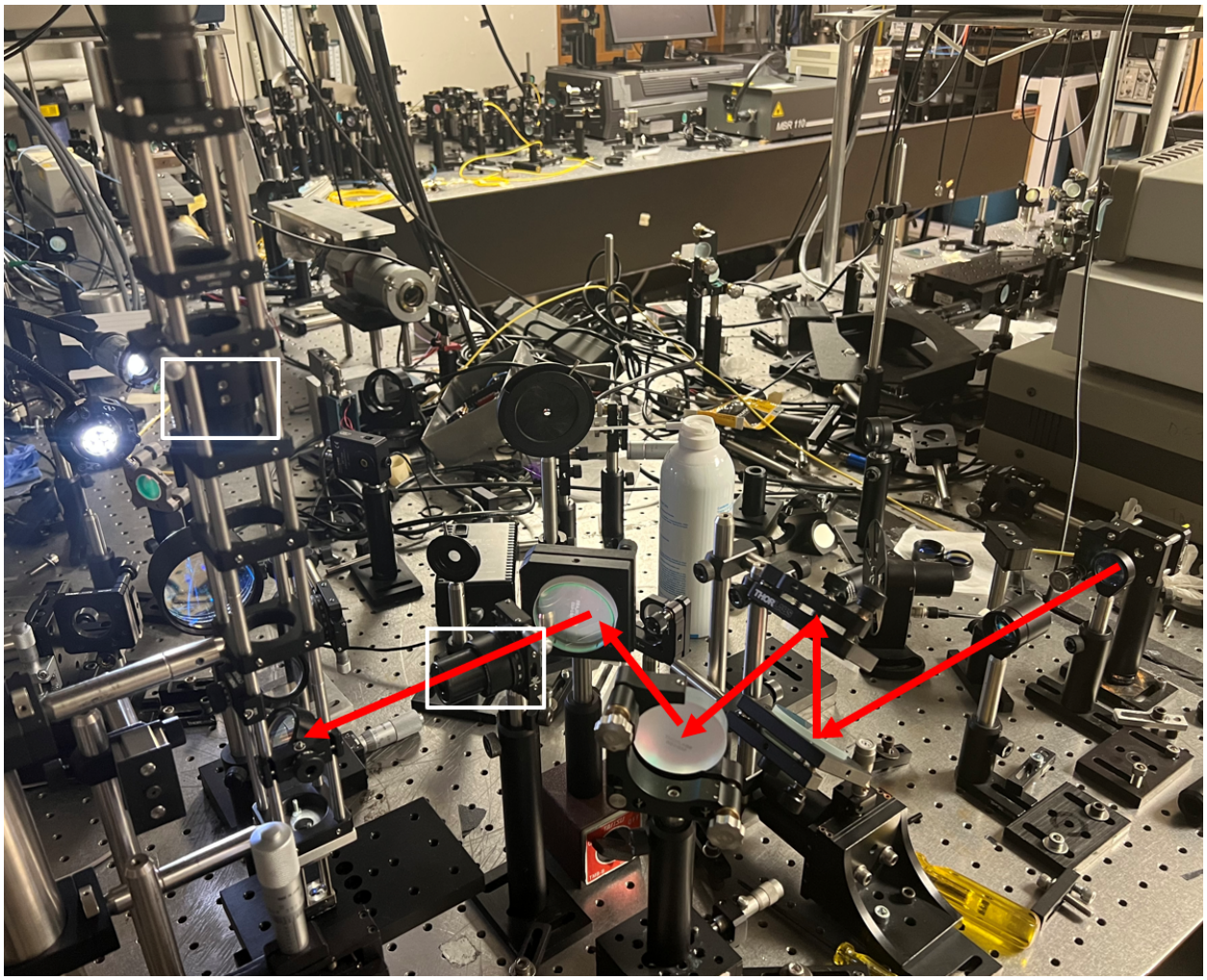

Figure 4: Experimental setup to verify the waveguides and input / output grating couplers. White light originates from the lamp on the left. Laser enters the setup from the yellow fiber optic cable on the right and follows the red path. Either the white light or the laser is directed to the sample at the bottom of the optical column, and the signal from the sample is collected by the CCD camera at the top of the optical column. The components outlined in white are polarizers.

Once the experimental setup had been sufficiently optimized such that the patterned sample had come into clear focus, the patterned sample was exchanged for a sample with an integrated waveguide and input / output grating couplers. The waveguide had a 90 degree bend in the middle. Additionally, the white light was turned off, and a near-infrared laser was routed to arrive at the sample instead. The position and angle of the near-infrared laser were adjusted until the laser landed on the input grating coupler. If aligned properly, the input grating coupler was expected to redirect the laser into the waveguide. The laser was expected to propagate through the waveguide until it arrived at the output grating coupler. The output grating coupler was then expected to redirect the laser away from the sample and towards the CCD camera. Ideally, the CCD camera would only detect the signal emerging from the output grating coupler. In practice, the CCD camera was likely to also detect a portion of the laser that scattered off the input grating coupler and did not enter the waveguide. To mitigate the scattering off the input grating coupler and isolate the signal from the output grating coupler, polarizers were inserted in the laser path before the sample and in the signal path between the sample and the CCD camera. In this fashion, the input laser had a particular polarization due to the effect of the first polarizer. The 90 degree bend caused the output signal to have a perpendicular polarization to the input laser. The second polarizer blocked signals whose polarization matched the input laser and passed signals whose polarization matched the output signal. However, some scattering from the input grating coupler still passed through the second polarizer because scattering resulted in random polarization. The experimental setup was optimized until the output signal was visible in the CCD camera image amidst the scattering of the input laser. Thus having seen evidence of the laser transmitting through the waveguide, the waveguide and input / output grating couplers had been verified to a satisfactory extent.

Results

Observing the quantum dot emission spectrum at all was a significant result. This signal was incredibly faint and hard to detect. It did not register on the available power meters in the slightest, suggesting that the signal had a power less than 1 μW. To observe this signal at the spectrometer, the signal collection path had to be optimized extensively. All other signals also had to be attenuated, which was achieved by inserting longpass filters into the signal collection path and turning off the ceiling lights in the lab while attempting to record the quantum dot emission spectrum. The number of spectral peaks in the quantum dot emission spectrum suggested that multiple quantum dots were being excited by the laser rather than just a single quantum dot.

Beyond observing the quantum dot emission spectrum, the most significant results obtained were the responses of the quantum dot emission spectrum to a variable applied bias voltage and a variable laser power. As the applied bias voltage increased from 0 V to 1.7 V in 0.5 V increments, the quantum dot emission spectrum was observed to shift to the left towards higher photon energies. This shift towards higher photon energies (and by extension, shorter photon wavelengths) is referred to as a blue shift because comparable shifts in the visible light regime tend to impart a blue hue to the emitter. The origin of this blue shift is a quantum mechanical phenomenon referred to as the optical Stark effect.[9] The optical Stark effect predicts that applying an electric field to a quantum well should induce a blue shift in the allowed transitions between energy levels, which agrees with the observations made in the lab. The observation of the optical Stark effect built confidence that the observed emission spectrum did, in fact, belong to the quantum dot. The response of the quantum dot emission spectrum to a variable applied bias voltage is shown in Figure 5.

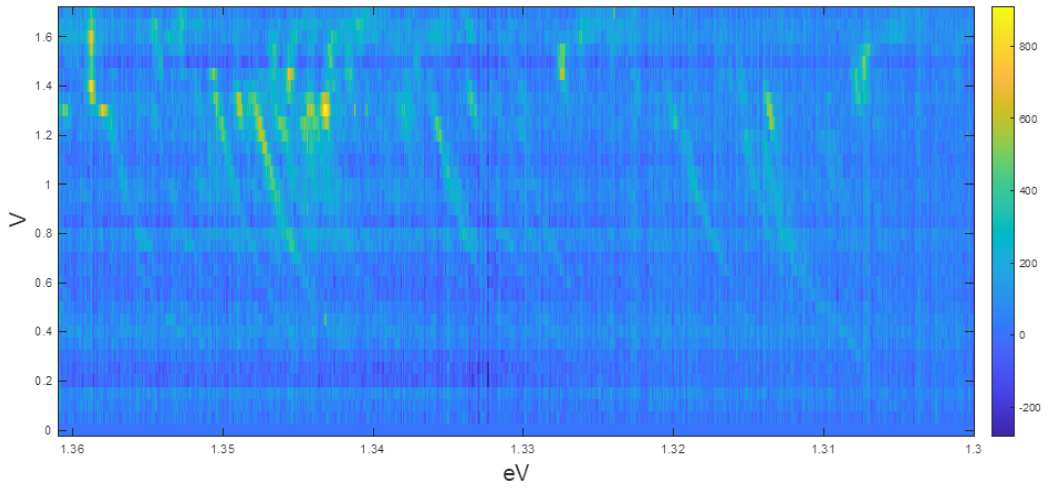

Figure 5: Quantum dot emission spectrum in response to a variable applied bias voltage. Laser is fixed at 890 nm wavelength and 170 μW power. As the applied bias voltage increases from 0 V to 1.7 V, the emission spectrum shifts to the left. This blue shift is the result of a quantum mechanical phenomenon known as the optical Stark effect. Observation of the Stark effect increases confidence that this emission spectrum does, in fact, belong to a quantum dot.

As the laser power increased from 0 μW to 1500 μW in 50 μW increments, the quantum dot emission spectrum was observed to increase linearly in intensity. This experimental observation agreed with theoretical expectations. As the laser power increased, different spectral peaks in the quantum dot emission spectrum increased linearly in intensity at different rates. These different rates were believed to correspond to exciton, biexciton, and triexciton excitement. The observation of the linear dependence of the quantum dot emission spectrum on laser power further built confidence that the observed emission spectrum did, in fact, belong to the quantum dot. The response of the quantum dot emission spectrum to a variable laser power is shown in Figure 6.

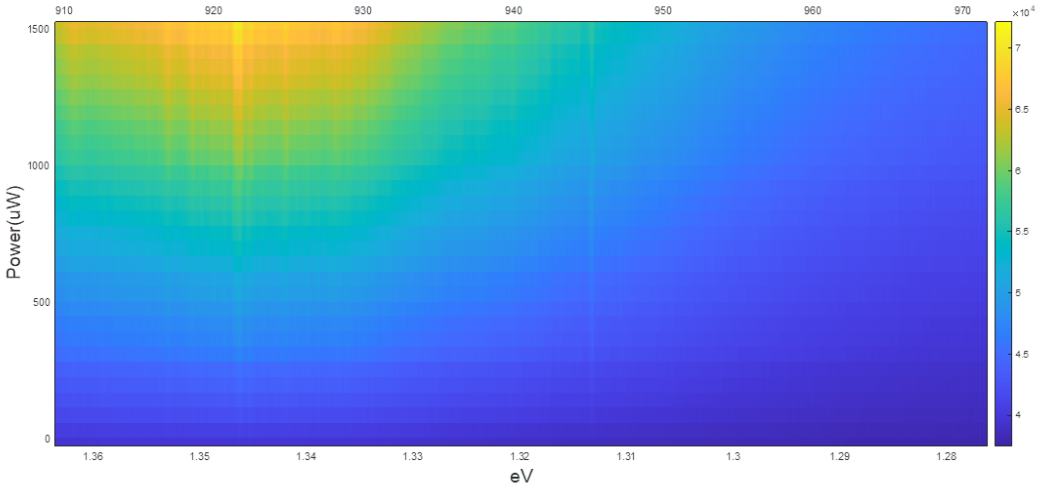

Figure 6: Quantum dot emission spectrum in response to a variable laser power. Applied bias voltage is fixed at 1.3 V. Laser wavelength is fixed at 890 nm. As the laser power increases from 0 μW to 1500 μW, the quantum dot emission spectrum increases linearly in intensity. The rate of this linear increase is different for different spectral peaks. These different rates are believed to correspond to exciton, biexciton, and triexciton excitement.

In addition to the quantum dot, the waveguides and input / output grating couplers were also verified. An experimental setup consisting of white light, a custom lens mount, and a portable CCD camera was optimized until a patterned sample came into focus in the CCD camera image. The patterns in this sample were approximately 100 microns across their longest dimension. Observing these patterns confirmed that the experimental setup was sound. The experimental setup was further optimized until the patterns in the sample were as clear as possible in the CCD camera image. The CCD camera image containing one of these patterns is shown in Figure 7.

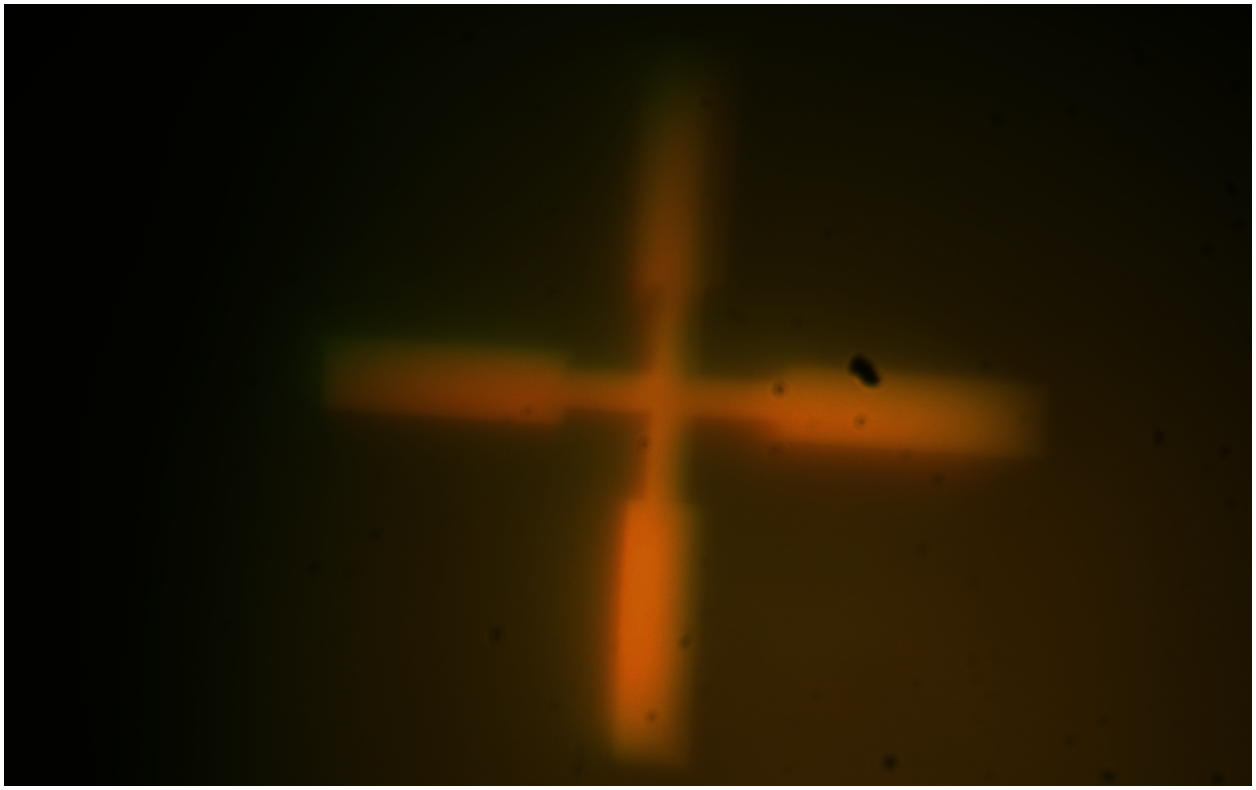

Figure 7: Patterned sample as captured by the CCD camera in the experimental setup shown in Figure 4. This pattern is approximately 100 microns across its longest dimension. Capturing a clear, crisp image of this pattern indicates that the experimental setup is sound and well-optimized.

Confident in the integrity of the experimental setup, the patterned sample was exchanged for a sample with an integrated waveguide and input / output grating couplers, and the white light was turned off in favor of a near-infrared laser. The near-infrared laser was directed at the input grating coupler, and the CCD camera captured the signal emerging from the output grating coupler (alongside the scattering of the laser off the input grating coupler). Using the CCD camera to measure the intensity of the signal coming from the output grating coupler and using a power meter to measure the power of the input laser, the efficiency of the waveguide was determined to be well under 1%. However, observing the signal emerging from

the output grating coupler nevertheless confirmed that the integrated waveguide and couplers had been fabricated properly and that the experimental setup was once again sound. The CCD camera image with the signal from the output grating coupler and the scattering from the input grating coupler are shown in Figure 8.

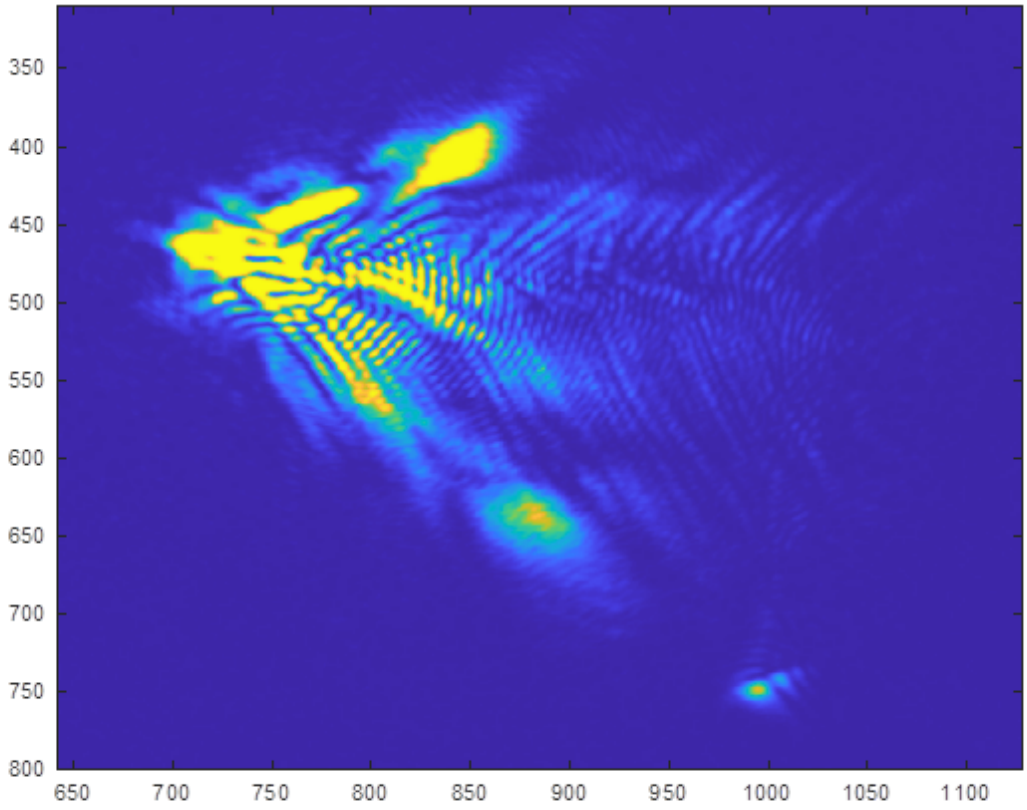

Figure 8: Integrated waveguide with a 90 degree bend as captured by the CCD camera in the experimental setup shown in Figure 4. The prominent splotch in the upper left corresponds to the scattering of the laser off the input grating coupler. The flecks in the bottom right correspond to the signal emerging from the output grating coupler. Using the CCD camera, the efficiency of the integrated waveguide was determined to be well under 1%.

Discussion and Future Work

The lab is still a ways away from being able to generate a photonic dimer. However, several crucial steps were made towards that goal over the course of this project. The lab has demonstrated the ability to design and optimize experimental setups to observe difficult-to-detect quantum phenomena, such as the emission spectrum of a quantum dot and the optical Stark effect. The lab has also demonstrated the ability to fabricate high-quality samples with detailed structures including patterns, integrated waveguides, and grating couplers. Lastly, the lab has become intricately familiar with important equipment and tools such as the spectrometer, cryostat, power meters, and fiber optic cables. These skills will undoubtedly translate to a broad variety of experiments in the future, and the successful development of these skills is an important result.

In addition to the development of critical skills, the lab has confirmed the correct operation of vital components of the planned experimental setup to eventually confirm the generation of a photonic dimer. These vital components include the quantum dot, waveguides, and input / output grating couplers. The lab observed the characteristic discrete emission spectrum of the quantum dot; observed the shifting of spectral peaks corresponding to the optical Stark effect; and observed evidence of exciton, biexciton, and triexciton excitement. The lab also observed the transmission of a near-infrared laser from an input grating coupler through a waveguide to an output grating coupler. These results give us great confidence that the quantum dot, waveguides, and input / output grating couplers will work as intended in the planned experimental setup.

Several components of the planned experimental setup remain to be verified. These unverified components include the photonic crystal, the phase modulator, and the Mach-Zehnder interferometer. The immediate next steps would be to verify the photonic crystal, which entails outsourcing work to a third party. This third party would be responsible for chirally coupling the quantum dot with the photonic crystal waveguide. The lab would then need to verify

this chiral coupling. If the quantum dot was chirally coupled with the photonic crystal waveguide successfully, then direct excitement of the quantum dot with a near-infrared laser should cause the quantum dot to emit a signal from one end of the photonic crystal waveguide and not the other end. This theoretical result would need to be experimentally observed. Next, the lab would determine the tolerance of the position of the quantum dot within the photonic crystal waveguide. After verifying the photonic crystal, the lab would verify the phase modulator to ensure an accurate response to an applied bias voltage. Only then would these components be assembled into a Mach-Zehnder interferometer, and attempts at generating a photonic dimer would begin. Although plans for this semester initially entailed verifying components such as the photonic crystal, work has been temporarily delayed pending the acquisition of specialized lab equipment including but not limited to single photon detectors.

Conclusion

During the course of this project, the lab made considerable progress towards the generation of a photonic dimer. Notably, the lab was able to design and carry out experiments to confirm the correct operation of the quantum dot, waveguides, and input / output grating couplers. Several other components (e.g., photonic crystal, phase modulator, Mach-Zehnder interferometer) must still be verified before attempts at generating a photonic dimer can begin. On a personal level, I feel like I greatly benefited from this experience. I appreciated the opportunity to do hands-on work in the field of experimental physics. I was especially happy to do work in the field of quantum optics. Quantum computing is a field that I am intensely interested in (hence my physics minor in addition to my computer engineering major), and I never imagined I would be able to do research that was so relevant to quantum computing during my undergraduate career. Although my plan directly after college is to enter the workforce, I may return to graduate school in the future to pursue my interest in quantum

computing even further. Whatever my future holds, I feel like this project has prepared me well with lab experience, practice in technical communication, and problem solving skills.

References

[1] J. Kim, Z. Croft, D. Steel, and P.-C. Ku, 'Controlled Phase Gate of Spin Qubits in Two Quantum-Dot Single-Photon Emitters', in *2021 Conference on Lasers and Electro-Optics (CLEO)*, 2021, pp. 1–2.

[2] Z. Chen, Y. Zhou, J.-T. Shen, P.-C. Ku, and D. Steel, 'Two-photon controlled-phase gates enabled by photonic dimers', *Physical Review A*, vol. 103, no. 5, p. 052610, 2021.

[3] J. Kim, D. Mastropietro, D. Steel, J.-T. Shen, and P.-C. Ku, 'Proposal for chip-scale generation and verification of photonic dimers', *Applied Physics Letters*, vol. 119, no. 22, 12 2021.

[4] J. Kim, Z. Croft, D. G. Steel, and P.-C. Ku, 'Optically Controlled Spin Gate Using GaN Quantum Dots', *ACS Photonics*, vol. 9, no. 5, pp. 1529–1534, 2022.

[5] P. Kok, W. J. Munro, K. Nemoto, T. C. Ralph, J. P. Dowling, and G. J. Milburn, 'Linear optical quantum computing with photonic qubits', *Reviews of modern physics*, vol. 79, no. 1, p. 135, 2007.

[6] J. Wang, F. Sciarrino, A. Laing, and M. G. Thompson, 'Integrated photonic quantum technologies', *Nature Photonics*, vol. 14, no. 5, pp. 273–284, 2020.

[7] L. Egan *et al.*, 'Fault-tolerant control of an error-corrected qubit', *Nature*, vol. 598, no. 7880, pp. 281–286, 2021.

[8] C. P. Williams, 'Quantum Gates', in *Explorations in Quantum Computing*, London: Springer London, 2011, pp. 51–122.

[9] A. Von Lehmen, D. S. Chemla, J. E. Zucker, and J. P. Heritage, ‘Optical Stark effect on excitons in GaAs quantum wells’, *Optics letters*, vol. 11, no. 10, pp. 609–611, 1986.

[10] “How does a spectrometer work?,” BWTek. [Online]. Available: https://bwtek.com/spectrometer-introduction/. [Accessed: 20-Apr-2023].

[11] “What is a cryostat?,” Oxford Instruments. [Online]. Available: https://andor.oxinst.com/learning/view/article/what-is-a-cryostat. [Accessed: 20-Apr-2023].

[12] J. Beaumont, ‘Physical Implementations’, University of Michigan, 2022.